Long-range empirical potential for the bcc structured transition metals

X. D. Dai, J. H. Li, and Y. Kong
Department of Materials Science and Engineering, Tsinghua University, Beijing 100084, China
(Received 26 September 2006; revised manuscript received 20 December 2006; published 6 February 2007)

A long-range empirical potential is developed for bcc transition metals in the present study and successfully applied to Fe, Mo, W, V, Nb, and Ta. It is found that the lattice constants, cohesive energies, elastic constants, vacancy formation energies, structural stabilities, and surface energies derived from the present model match well with the experimental values or *ab initio* calculations. More importantly, the energies and forces represented by the present model can smoothly go to zero at cutoff radius, thus completely avoiding the unphysical behaviors to emerge in simulations.

DOI: 10.1103/PhysRevB.75.052102 PACS number(s): 61.43.Bn, 61.82.Bg, 81.05.Bx, 02.70.Ns

In 1984, Finnis and Sinclair (FS) developed the first short-range *n*-body potential for bcc transition metals,[1] which can reasonably reproduce the properties of the bcc metals yet exhibits a "soft" feature when the atomic volume is less than the equilibrium one. Five years later, Johnson proposed an analytic embedded atom method (EAM) potential for bcc transition metals,[2] and successively, Adams developed another EAM potential for bcc metals.[3] Nevertheless, both potentials are still short-range potentials. Later, other researchers, such as Pasianot, Doyama, Zhang, and Dai,[4–7] proposed several short-range potentials for bcc metals. Although they are different in their details, they are actually the modified forms either of EAM or of FS models. The short-range models have an apparent problem, i.e., they frequently produce the same calculated potential energy for the metastable fcc and ideal hcp structures.[7] In order to overcome the problem, researchers have tried to construct new models for bcc metals. For instance, by considering the angular contributions, Baskes *et al.* proposed a modified EAM (MEAM) model for bcc metals.[8] The MEAM model resolves the problem mentioned above, however, it also brings more application problems at the same time, e.g., the potential parameters related to the angular factors make it difficult to apply the model to the disordered metal systems. In the tight-binding (TB) theory, Finnis has mentioned that adopting a high-order moment approximation could improve the capability of the TB potential in predicting the structural stability,[9] however, it is difficult to obtain an analytic form in practice. Besides, the short-range models for bcc metals also frequently encounter another problem, i.e., the energy generally cannot smoothly go to zero at the cutoff radius and more seriously the forces will make a jump at the cutoff radius. (See the curves in Fig. 1.) A large number of these events will spoil the energy conservation or lead to some unphysical behaviors in simulations. To avoid the problem, a truncation function should be introduced, like Johnson, Adams, and Guellil have done.[2,3,10] Inspecting the curves derived by Johnson's EAM potential in Fig. 1, one sees that although a cubic truncation function has been adopted, the problem has not yet been solved. Naturally, if the potential can overcome the problem without adopting any truncation function, the computation program will significantly be simplified and much computer time can be saved. In order to resolve the above two problems related to the short-range potentials, we propose, in the present work, a long-range empirical potential (LREP) for the bcc transition metals under the framework of the second-moment approximation of the tight-binding (TB-SMA) theory.

According to the TB-SMA theory,[11] the total potential energy E_i of an atom i is expressed as

$$E_{\mathrm{i}} = \frac{1}{2}\sum_{\mathrm{j}\neq\mathrm{i}} \phi(r_{\mathrm{ij}}) - \sqrt{\sum_{\mathrm{j}} \varphi(r_{\mathrm{ij}})}, \tag{1}$$

where r_{ij} is the distance between atoms i and j of the system at equilibrium state. In Eq. (1), $\frac{1}{2}\Sigma_{\mathrm{j}\neq\mathrm{i}}\phi(r_{\mathrm{ij}})$ and $-\sqrt{\Sigma_{\mathrm{j}}}\varphi(r_{\mathrm{ij}})$ are the repulsive pair term and *n*-body term, respectively. $\phi(r_{\mathrm{ij}})$ is expressed by a Born-Mayer type in the original TB-SMA scheme, while in the proposed LREP model, it is expressed by a polynomial as follows:

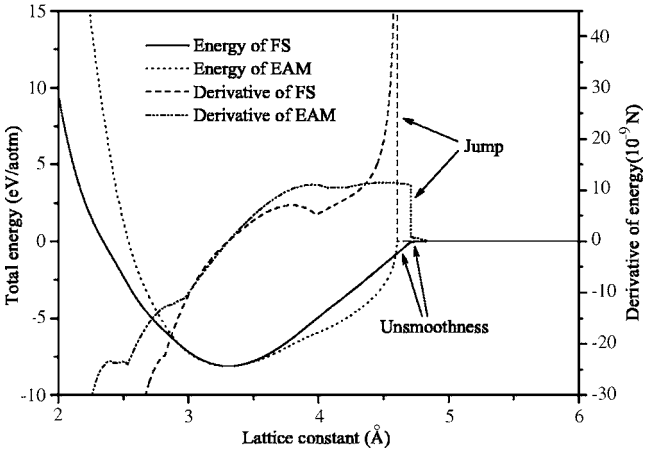

FIG. 1. Total energy and its first derivative as a function of lattice constant calculated from the FS potential (Ref. 1) and EAM potential (Ref. 2) for bcc Ta.

$$\phi(r_{ij}) = \begin{cases} (r_{ij} - r_{c1})^m (x_0 + x_1 r_{ij} + x_2 r_{ij}^2 + x_3 r_{ij}^3 + x_4 r_{ij}^4), & r_{ij} \le r_{c1}, \\ 0, & r_{ij} > r_{c1}, \end{cases} \tag{2}$$

where r_{c1} is a cutoff radius and x_0, x_1, x_2, x_3, and x_4 are the potential parameters to be fitted. In the proposed LREP model, $\varphi(r_{ij})$ is expressed by

$$\varphi(r_{ij}) = \begin{cases} \alpha(r_{ij} - r_{c2})^n \exp\left[-\beta\left(\frac{r_{ij}}{r_0} - 1\right)\right], & r_{ij} \le r_{c2}, \\ 0, & r_{ij} > r_{c2}, \end{cases} \tag{3}$$

where r_{c2} is also a cutoff radius and r_0 is the first-neighbor distance. α and β are two adjustable parameters, i.e., the potential parameters. If necessary, r_{c1}, r_{c2}, and r_0 can also be treated as free parameters in the fitting procedure. m and n are generally adopted with integer values and can be adjustable according to the specific element. From the forms expressed in Eqs. (2) and (3), one sees clearly that if $m>3$ and $n>3$, the terms of $(r_{ij}-r_{c1})^m$ and $(r-r_{c2})^n$ can ensure $\phi(r_{ij})$, $\varphi(r_{ij})$ and their first derivatives smoothly go to zero at the cutoff radii. In other words, the total energy and force in the present potential can keep continuous and smooth in the whole calculated range and thus completely remove the cutoff problem taking place in the traditional short-range potentials.

For the pure bcc transition metals, the potential parameters are determined by fitting their basic physical properties obtained from experiments, i.e., the cohesive energy, lattice constant, elastic constants, and vacancy formation energy. Besides, when a metal is in equilibrium, the first derivative dE of potential energy and the stress σ of each unit cell should equate to zero, so $dE(a)|_{a=a_0}=0$ and $\sigma(a)|_{a=a_0}=0$ have been regarded as the two fitting conditions in the present study so as to confirm the equilibrium state of a structure. Different from the short-range potential, we adopted the longer cutoff radii for all the bcc metals, i.e., $r_{c1}>r_3$ and $r_{c2}>r_6$, where r_3 and r_6 are the third- and sixth-neighbor distances, respectively. Table I displays all the fitted potential parameters for six selected bcc metals, i.e., Fe, Mo, W, V, Nb, and Ta. It is noted that the reproduced properties, i.e., lattice constant, cohesive energy, elastic constants, and vacancy formation energy, completely match with their experimental values. In addition, the derivative and stress are very small, indicating that the fitted structures of the six studied metals are very close to the equilibrium states.

TABLE I. The potential parameters of six bcc transition metals derived in present study. $m=4$, $n=6$, r_{c1}, r_{c2}, and r_0 expressed in Å. x_0, x_1, x_2, x_3, x_4, and α are expressed in 10 eV Å^{-m}, 10 eV Å^{-m-1}, 10 eV Å^{-m-2}, eV Å^{-m-3}, 10^{-1} eV Å^{-m-4}, and 10^{-3} eV^2 Å^{-n}, respectively.

	Fe	Mo	W	V	Nb	Ta
r_{c1}	4.540	4.700	4.800	4.650	5.020	5.079
r_{c2}	6.600	6.600	6.800	6.700	6.700	6.700
x_0	0.6676	2.9973	2.8576	0.7396	0.8503	0.6618
x_1	−1.0212	−4.1933	−3.9805	−1.0602	−1.1104	−0.8748
x_2	0.5893	2.1966	2.0772	0.5730	0.5462	0.4370
x_3	−1.5190	−5.0972	−4.8066	−1.3743	−1.1905	−0.9714
x_4	1.4745	4.4138	4.1581	1.2275	0.9645	0.8081
r_0	2.4855	2.7280	2.7366	2.6241	2.8579	2.8579
β	−1.5958	−0.1903	−1.3373	1.8017	1.6823	0.1175
α	0.3479	1.4774	1.7151	0.8295	2.9256	3.1530

To evaluate the relevance of the constructed potentials, we first calculate the energies of the metastable structures, i.e., the fcc and ideal hcp structures of the six bcc metals at equilibrium by using the constructed potentials. The fcc and hcp structures are first optimized using the constructed potentials and then the potential energies, lattice constants of the metastable structures, are calculated. It is noted that the atomic volume is allowed to vary during the present optimization, differing from other constant-atomic-volume methods, in which the atomic volume is assumed to be constant in various structures. Table II shows the energy differences between the bcc, fcc, and ideal hcp structures predicted by the LREP model for the six bcc metals. For comparison, the results derived from the *ab initio* calculations and the results calculated from the FS and EAM potentials are also listed in Table II. In the present study, the *ab initio* calculations are carried out using the well-established Vienna *ab initio* simulation package (VASP).[12,13] In the calculation, the projector augmented wave (PAW) method[14] and the plane-wave basis together with fully nonlocal Vanderbilt-type ultrasoft pseudopotentials are employed.[15] The exchange and correlation items are described by the generalized-gradient approximation (GGA) proposed by Perdew and Wang.[16] The integration in the Brillouin zone is done in a mesh of $11\times11\times11$

TABLE II. Energy differences ΔE (meV) between three simple structures for Fe, Mo, W, V, Nb, and Ta, respectively. The results of FS and EAM are calculated from the potentials in Refs. 1 and 2. The values of c/a for all hcp structures are 1.632 99.

		Fe	Mo	W	V	Nb	Ta
$\Delta E_{bcc\to fcc}$	LREP	48	486	364	144	209	188
	Ab initio	124	423	478	255	326	243
$\Delta E_{bcc\to hcp}$	LREP	75	491	425	151	214	199
	Ab initio	62	460	563	292	351	314
$\Delta E_{fcc\to hcp}$	LREP	27	6	61	7	5	5
	Ab initio	−61	37	84	36	24	71
	FS	0	0	0	0	0	0
	EAM	0	0	0	0	0	0

TABLE III. Surface energies (J/m^2) of three low-index faces for Fe, Mo, W, V, Nb, and Ta, respectively.

		Fe	Mo	W	V	Nb	Ta
(110)	EAM[a]	1.535	2.127	2.599	1.683	1.807	1.800
	MEAM[b]	2.356	2.885	3.427	2.636	2.490	2.778
	LREP	1.717	2.229	2.967	1.676	1.792	1.909
	Expt.[c]	1.683	2.019	2.275	1.827	1.859	2.019
(100)	EAM[a]	1.685	2.284	2.809	1.831	1.968	1.990
	MEAM[b]	2.510	3.130	3.900	2.778	2.715	3.035
	LREP	1.899	2.459	3.223	1.929	2.101	2.223
	Expt.[c]	2.388	2.868	3.221	2.596	2.628	2.868
(111)	MEAM[b]	2.668	3.373	4.341	2.931	2.923	3.247
	LREP	2.076	2.803	3.628	2.161	2.343	2.480

[a]Reference 10.
[b]Reference 8.
[c]Reference 19.

special k points determined according to the Monkhorst-Pack scheme, as such integration is proved to be sufficient for the computation of the simple structures.[17] From Table II, one sees clearly that the values of $\Delta E_{\mathrm{bcc}\rightarrow\mathrm{fcc}}$ and $\Delta E_{\mathrm{bcc}\rightarrow\mathrm{hcp}}$ predicted by the present model match well with those derived from the *ab initio* calculations. Both the present model and *ab initio* calculations indicate that the bcc structure has the lowest potential energy, reflecting well the fact that the equilibrium states of the six studied metals are in bcc structures. As for the relative stability of the metastable fcc and ideal hcp structures, the values of $\Delta E_{\mathrm{fcc}\rightarrow\mathrm{hcp}}$ predicted by the FS and EAM potentials are equal to zero, indicating that the two traditional short-range models cannot distinguish the energy difference between the two structures. Inspecting the values of $\Delta E_{\mathrm{fcc}\rightarrow\mathrm{hcp}}$ predicted by the LREP model, one sees that the energy differences of Mo, W, V, Nb, and Ta are qualitatively match with those derived from *ab initio* calculations. The only exception is that of Fe, showing an opposite sign to that derived from the *ab initio* calculations. The exceptional result possibly comes from the special property of element Fe, i.e., its ferromagnetic property.

Based on the constructed potentials, we also calculated the surface energies for the six bcc transition metals. Regarding the surface energy calculation, the results obtained by Foiles have proven that the relaxation would only result in a minor reduction to the surface energy and would not greatly affect the calculation results.[18] We therefore only calculated the unrelaxed surface energies for three low-index faces, i.e., (110), (100), and (111). The results calculated by the LREP model, by EAM potential, and by MEAM potential, respectively, as well as the experimental values are all listed in Table III. It can be seen that for all the studied metals, the energy sequence of these faces is completely consistent with the results obtained by various computation methods, i.e., the close-packed (110) face has the lowest energy, followed by the (100) and then the (111) faces, which are in good agreement with the experimental observations.[20,21] In general, for the (110) face, the results derived from the LREP model and EAM potential are closer to the experimental values than those obtained from the MEAM potential. For the (100) face, the results from the MEAM and those from the LREP model, respectively, show a little greater and less than the experimental values, while those from the EAM potential show the maximum departure comparing with the experimental values. In short, the surface energies of the six bcc metals derived from the LREP model match well with the experimental results, suggesting an apparent improvement comparing with those calculated from the empirical short-range potentials proposed previously.

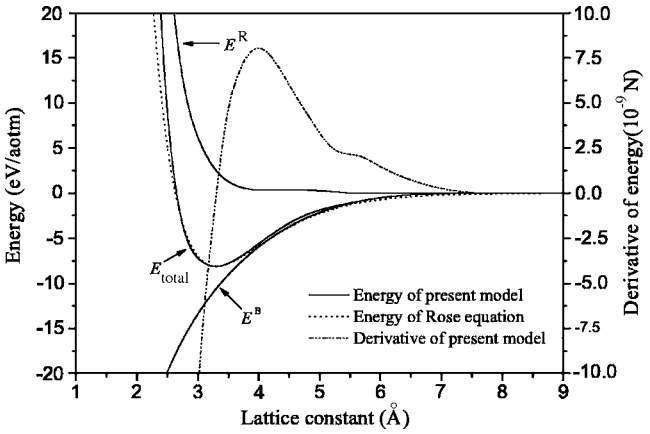

FIG. 2. Total energy (E_{total}), repulsive term (E^{R}), n-body term (E^{B}), and the first derivative of total energy as a function of lattice constant for bcc Ta.

Another approach to evaluate the relevance of the constructed potential is to derive the equation of state (EOS) from the potential and then compare it with the EOS obtained from theory or from experiment. As an example, the EOS, i.e., the potential energy as a function of the lattice

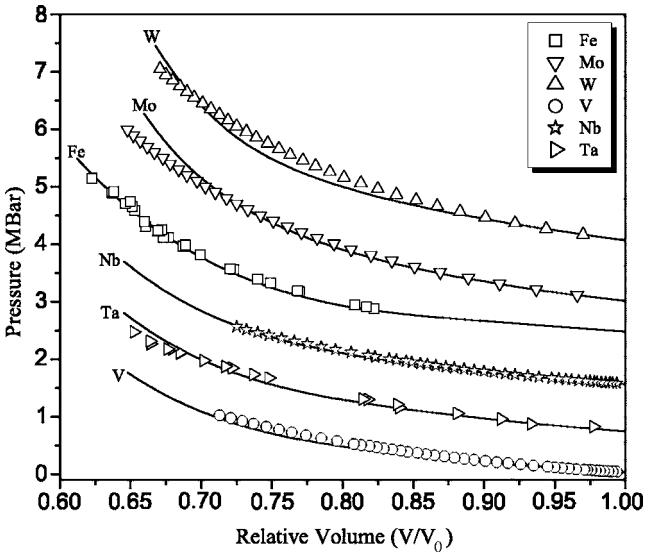

FIG. 3. The relationships of pressure vs relative volume obtained from the present model and experiments, respectively, for Fe, Mo, W, V, Nb, and Ta. The solid curves are from the present model, and the scattered points are from experiments. For each curve, the value of the cross point with the vertical axis is zero. The experimental values are from Refs. 23–26.

constant for Ta, is therefore derived from the LREP model and the Rose equation,[22] respectively, and shown in Fig. 2. One sees from Fig. 2 that the repulsive term, *n*-body term, and the total energy derived from the LREP model can keep smooth in the whole calculated range, and that the calculated total energy matches well with that derived from the Rose equation, indicating that the proposed LREP model can reasonably describe the interatomic interaction of a system even in a far from equilibrium state. In addition, the derivative of the total energy as a function of the lattice constant is also derived from the LREP model and shown in Fig. 2. From Fig. 2, one sees that the derivative curve derived from the LREP model is smooth in the whole calculated range, indicating that the proposed LREP model can avoid the unphysical behaviors to emerge in simulations. Furthermore, we also calculated the relationships of the pressure vs volume for the six bcc metals based on the LREP model and compared them with their respective experimental values in Fig. 3. It is clearly shown that the agreement between the calculated results and experimental values is good, indicating that the LREP model can reasonably describe the *P*-*V* relationships in the bcc metals even at a nonequilibrium state.

In summary, a LREP model has been developed for the bcc transition metals and the LREP model can satisfactorily reproduce the properties of the bcc metals as well as can reasonably describe the interatomic interactions in the bcc metals. Unlike the MEAM model or high-order-moment TB models, the proposed LREP model has a simple analytic form and can be widely applied in the metals, alloys (including their order and disordered states), and in the large-scale simulations.

The authors are grateful for the financial support from the National Natural Science Foundation of China (Grant No. 50531040), The Ministry of Science and Technology of China (Grant No. 2006CB605201), and the Administration of Tsinghua University.

*Corresponding author. Electronic address: daixd03@mails.tsinghua.edu.cn

[1] M. W. Finnis and J. E. Sinclair, Philos. Mag. A **50**, 45 (1984).
[2] R. A. Johnson and D. J. Oh, J. Mater. Res. **4**, 1195 (1989).
[3] J. B. Adams and S. M. Foiles, Phys. Rev. B **41**, 3316 (1990).
[4] R. Pasianot, D. Farkas, and E. J. Savino, Phys. Rev. B **43**, 6952 (1991).
[5] M. Doyama and Y. Kogure, Comput. Mater. Sci. **14**, 80 (1999).
[6] B. W. Zhang, Y. F. Ouyang, S. Z. Liao, and Z. P. Jin, Physica B **262**, 218 (1999).
[7] X. D. Dai, Y. Kong, J. H. Li, and B. X. Liu, J. Phys.: Condens. Matter **18**, 4527 (2006).
[8] Byeong-Joo Lee, M. I. Baskes, Hanchul Kim, and Yang Koo Cho, Phys. Rev. B **64**, 184102 (2001).
[9] M. Finnis, *Interatomic Forces in Condensed Matter* (Oxford University Press, New York, 2003).
[10] A. M. Guellil and J. B. Adams, J. Mater. Res. **7**, 639 (1992).
[11] V. Rosato, M. Guillope, and B. Legrand, Philos. Mag. A **59**, 321 (1989).
[12] G. Kresse and J. Hafner, Phys. Rev. B **47**, 558 (1993).
[13] G. Kresse and J. Furthmuller, Phys. Rev. B **54**, 11169 (1996).
[14] G. Kresse and D. Joubert, Phys. Rev. B **59**, 1758 (1999).
[15] D. Vanderbilt, Phys. Rev. B **41**, 7892 (1990).
[16] J. P. Perdew and Y. Wang, Phys. Rev. B **45**, 13244 (1992).
[17] J. B. Liu, Z. C. Li, B. X. Liu, G. Kresse, and J. Hafner, Phys. Rev. B **63**, 132204 (2001).
[18] S. M. Foiles, Surf. Sci. **191**, 779 (1987).
[19] W. R. Tyson and W. A. Miller, Surf. Sci. **62**, 267 (1977).
[20] B. E. Sundquist, Acta Metall. **12**, 67 (1964).
[21] H. E. Grenga and R. Kumar, Surf. Sci. **61**, 283 (1976).
[22] J. H. Rose, J. R. Smith, F. Guinea, and J. Ferrante, Phys. Rev. B **29**, 2963 (1984).
[23] R. Kinslow, *High-Velocity Impact Phenomena* (Academic, New York and London, 1970).
[24] R. S. Hixson and J. N. Fritz, J. Appl. Phys. **71**, 1721 (1992).
[25] D. E. Gray, *American Institute of Physics Handbook* (McGraw-Hill, New York, 1972).
[26] H. Cynn and C.-S. Yoo, Phys. Rev. B **59**, 8526 (1999).